



Universiteit  
Leiden  
The Netherlands

## A photoswitchable macrocycle controls anion-templated pseudorotaxane formation and axle relocalization

Jong, J. de; Siegler, M.A.; Wezenberg, S.J.

### Citation

Jong, J. de, Siegler, M. A., & Wezenberg, S. J. (2023). A photoswitchable macrocycle controls anion-templated pseudorotaxane formation and axle relocalization. *Angewandte Chemie (International Edition)*, 63(4). doi:10.1002/anie.202316628

Version: Publisher's Version

License: [Creative Commons CC BY 4.0 license](https://creativecommons.org/licenses/by/4.0/)

Downloaded from: <https://hdl.handle.net/1887/3716106>

**Note:** To cite this publication please use the final published version (if applicable).

# A Photoswitchable Macrocyclic Host Controls Anion-Templated Pseudorotaxane Formation and Axle Relocalization

Jorn de Jong, Maxime A. Siegler, and Sander J. Wezenberg\*

**Abstract:** Important biological processes, such as signaling and transport, are regulated by dynamic binding events. The development of artificial supramolecular systems in which binding between different components is controlled could help emulate such processes. Herein, we describe stiff-stilbene-containing macrocycles that can be switched between (*Z*)- and (*E*)-isomers by light, as demonstrated by UV/Vis and <sup>1</sup>H NMR spectroscopy. The (*Z*)-isomers can be effectively threaded by pyridinium halide axles to give pseudorotaxane complexes, as confirmed by <sup>1</sup>H NMR titration studies and single-crystal X-ray crystallography. The overall stability of these complexes can be tuned by varying the templating counteranion. However, upon light-induced isomerization to the (*E*)-isomer, the threading capability is drastically reduced. The axle component, in addition, can form a heterodimeric complex with a secondary isophthalamide host. Therefore, when all components are combined, light irradiation triggers axle exchange between the macrocycle and this secondary host, which has been monitored by <sup>1</sup>H NMR spectroscopy and simulated computationally.

## Introduction

In biological systems, external stimulus-controlled association and dissociation between (sub)components is pivotal to many processes, including signal transduction,<sup>[1]</sup> and molecular motion and transport.<sup>[2]</sup> These processes have sparked interest in the development of artificial host–guest complexes in which binding properties can be modulated.<sup>[3]</sup> In this respect, the use of light as the stimulus is advantageous as it does not produce any waste products. Further, the incorporation of molecular photoswitches into macrocyclic

hosts has proven to be a particularly promising approach to achieve this goal, owing to the large shape changes that are induced upon photochemical isomerization.<sup>[4]</sup>

The threading of macrocyclic hosts onto axle-like molecules has culminated into interpenetrated (pseudorotaxane) and interlocked (rotaxane, catenane) structures, which are particularly interesting for creating artificial molecular machines and pumps.<sup>[5,6]</sup> Despite the large changes in binding affinity reported for photoswitchable macrocycles, assembly of pseudorotaxanes is usually controlled through incorporation of a light-responsive moiety into the axle rather than the macrocyclic ring.<sup>[7,8]</sup> An exception was reported by the group of Hirose, who demonstrated control of the (de)threading process of a pseudorotaxane formed from a bis(anthracene) crown ether and a dibenzylammonium axle.<sup>[9]</sup> This process was, however, not yet very effective, given the small (3-fold) change in stability constant upon photodimerization of anthracene. Improved control—toward more complex functions—is thus highly desired, not only with respect to photoswitching of the macrocyclic ring, but also in terms of additional means to fine-tune the binding strength.

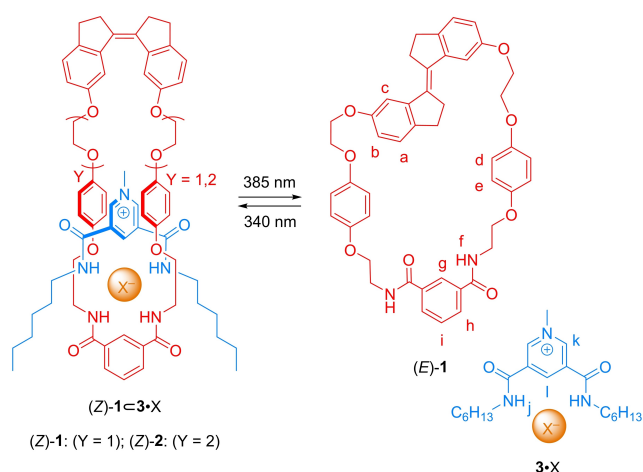
To address these issues, we became interested in using anion-templated pseudorotaxane structures, which were extensively developed by the group of Beer.<sup>[10,11]</sup> In one of their earliest designs, an isophthalamide-containing macrocycle was threaded by a pyridinium bis-amide axle, with its halide counteranion hydrogen-bonded in between the components.<sup>[11a,b]</sup> As such, the overall stability of the pseudorotaxane structure can be tuned by varying this counteranion. We envisioned that incorporation of a stiff-stilbene photoswitch<sup>[12,13]</sup> into the macrocycle would enable effective control of the threading process by light. So far, to our best knowledge, control by light over anion-templated assembly of pseudorotaxane structures has not been demonstrated.

Herein, we describe anion-templated pseudorotaxane formation with stiff-stilbene based macrocycles **1** and **2** (Scheme 1), which contract and expand in response to a light stimulus. Where the (*Z*)-isomers are threaded by pyridinium halide axles **3-X** (X = Cl, Br, I), photoisomerization to the respective (*E*)-isomers triggers dissociation of this axle component. As an additional feature, the axle can then be taken up by a secondary isophthalamide host to form an anion-bound heterodimeric complex. This light-controlled guest exchange between host molecules opens opportunities for communicating chemical systems,<sup>[14,15]</sup> to enable processing of signals and information. Further, this control of the (de)threading process by geometrical changes in the macro-

[\*] J. de Jong, Dr. S. J. Wezenberg  
 Leiden Institute of Chemistry, Leiden University  
 Einsteinweg 55, 2333 CC Leiden (The Netherlands)  
 E-mail: s.j.wezenberg@lic.leidenuniv.nl

Dr. M. A. Siegler  
 Department of Chemistry, Johns Hopkins University  
 3400 N. Charles St., Baltimore, MD 21218 (USA)

© 2023 The Authors. Angewandte Chemie International Edition published by Wiley-VCH GmbH. This is an open access article under the terms of the Creative Commons Attribution License, which permits use, distribution and reproduction in any medium, provided the original work is properly cited.

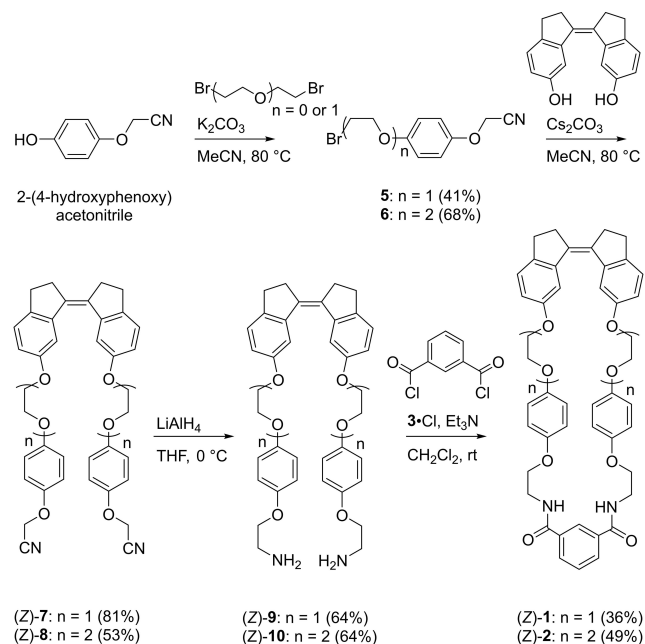


**Scheme 1.** Representation of light-promoted (de)threading of stiff-stilbene-based macrocycles (Z)-1 and (Z)-2 by pyridinium halide axes (X=Cl, Br, I).

cycle could be used to move it directionally along a nonsymmetric axle.<sup>[5,6]</sup>

## Results and Discussion

Macrocycles **1** and **2** were prepared as their (Z)-isomers following the synthetic route outlined in Scheme 2.<sup>[16]</sup> Starting from previously reported 2-(4-hydroxyphenoxy)acetonitrile,<sup>[17]</sup> alkylation with an excess of either 1,2-dibromoethane or bis(2-bromoethyl) ether under basic conditions afforded alkyl bromides **5** and **6**, respectively. These products were then coupled with (Z)-stiff-



**Scheme 2.** Synthesis of stiff-stilbene-based macrocycles (Z)-1 and (Z)-2.

stilbene-6,6' diol, which was synthesized according to a procedure from the group of Boulatov,<sup>[18]</sup> to obtain bis-nitriles (Z)-7 and (Z)-8. Subsequent reduction of the nitrile groups using lithium aluminium hydride resulted in formation of bis-amines (Z)-9 and (Z)-10, which were cyclized with isophthaloyl chloride via an amidation reaction to give the desired macrocycles. This cyclization was templated by pyridinium chloride axle **3-Cl** following a protocol developed by the group of Beer.<sup>[11e]</sup>

The photoswitching behavior was initially investigated by UV/Vis spectroscopy in dichloromethane (Figure 1A,B). Absorption maxima were found around  $\lambda=350$  and 360 nm for both (Z)-1 and (Z)-2. In either case, irradiation with 385 nm light resulted in an absorption increase and a slight hypsochromic shift of the maxima and the longer wavelength absorption, which is characteristic for Z→E isomerization of stiff-stilbene.<sup>[12,13]</sup> When the same sample was subsequently irradiated with 340 nm light, these spectral changes partially reversed, illustrative of isomerization back to the (Z)-isomer. The samples were irradiated until the photostationary states (PSS) had been reached and, at both irradiation wavelengths, clear isosbestic points were observed, indicating a unimolecular process (Figures S17–S20 in the Supporting Information). Importantly, 385/340 nm irradiation could be repeated multiple times without significant signs of fatigue (Figure 1C,D).

Next, the photoisomerization process was monitored by <sup>1</sup>H NMR spectroscopy allowing determination of the PSS ratios (Figures S21–S22 in the Supporting Information). When solutions of (Z)-1 and (Z)-2 in dichloromethane-*d*<sub>2</sub> were exposed to 385 nm light, new signals appeared that could be ascribed to the corresponding (E)-isomers. Again, subsequent 340 nm irradiation led to the reverse spectral changes showing recovery of the (Z)-isomer. By <sup>1</sup>H NMR signal integration it was determined that the PSS<sub>385</sub> mixtures

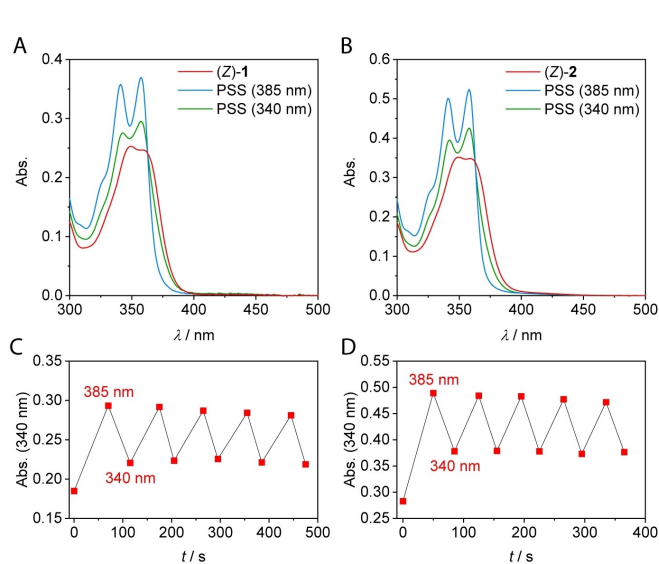


**Figure 1.** UV/Vis spectral changes of (Z)-1 (A) and (Z)-2 (B) upon consecutive irradiation with 385 nm and 340 nm light ( $c=2.0\times 10^{-5}$  M in dichloromethane) and change in absorption at 340 nm during 385/340 nm irradiation cycles (C,D).

contained >95 % of the (*E*)-isomer, whereas the PSS<sub>340</sub> (*E*/*Z*) ratios were 55:45 and 48:52 for **1** and **2**, respectively.

After having established that the macrocycles can be isomerized by light, their threading with pyridinium axle **3** having different halide counteranions (i.e., Cl<sup>-</sup>, Br<sup>-</sup>, I<sup>-</sup>) was studied by <sup>1</sup>H NMR spectroscopy in water-saturated chloroform-*d*.<sup>[19]</sup> In all cases, stepwise addition of the axle to the (*Z*)-isomers led to major changes in the <sup>1</sup>H NMR spectrum, which were indicative of the formation of a pseudorotaxane structure (Figure 2 and Figures S23–S28 and S37–S42 in the Supporting Information).<sup>[11]</sup> For example, when **3**-Cl was added to (*Z*)-**1**, the aromatic singlet (H<sub>g</sub>) and NH signal (H<sub>i</sub>) of the isophthalamide part of the macrocycle experienced a pronounced downfield shift as a result of their hydrogen-bonding interaction with the chloride anion (from  $\delta=7.97$  to 9.08 ppm and from  $\delta=6.87$  to 8.51 ppm, respectively). Furthermore, the hydroquinone signals (H<sub>d,e</sub>), which appeared as singlet ( $\delta=6.77$  ppm) for (*Z*)-**1** alone, shifted upfield and split into two signals ( $\delta=6.41$  and 6.19 ppm). At the same time, the amide (H<sub>j</sub>) and aromatic protons (H<sub>k,i</sub>) of the axle became more shielded as a result of sharing the counteranion with (*Z*)-**1** (the chemical shift of H<sub>i</sub>, H<sub>j</sub> and H<sub>k</sub> changed from  $\delta=10.71$ , 9.63 and 9.24 ppm to  $\delta=10.68$ , 9.60 and 9.19 ppm, respectively).

Similar chemical shift changes upon combining this pyridinium halide axle with structurally related (non-switchable) macrocycles were described by Beer and co-workers,<sup>[11a-c]</sup> thus supporting the formation of an interpenetrated pseudorotaxane structure. <sup>1</sup>H NMR dilution experiments performed with the pyridinium halide axles did not show any noteworthy chemical shift changes, on which

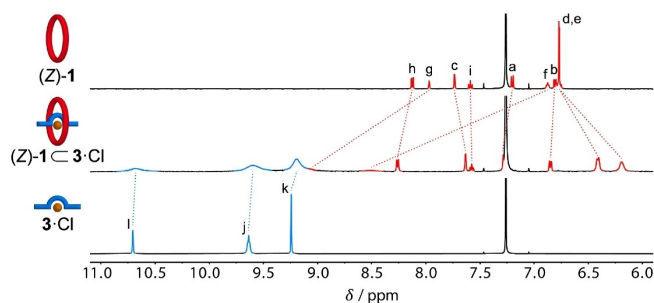


**Figure 2.** <sup>1</sup>H NMR spectra of (*Z*)-**1** (1.0 mM, top), **3**-Cl (5.0 mM, bottom), and a mixture of both components (middle) in chloroform-*d* saturated with water; see Scheme 1 for the lettering assignments.

**Table 1:** Association constants ( $K_a$ ) of macrocycles **1** and **2** with pyridinium halide axles **3**•X in chloroform-*d*/sat. H<sub>2</sub>O.<sup>[a]</sup>

Axle	( <i>Z</i> )- <b>1</b> [M <sup>-1</sup> ]	( <i>E</i> )- <b>1</b> [M <sup>-1</sup> ]	$K_{a,Z}/$ $K_{a,E}$	( <i>Z</i> )- <b>2</b> [M <sup>-1</sup> ]	( <i>E</i> )- <b>2</b> [M <sup>-1</sup> ]	$K_{a,Z}/$ $K_{a,E}$
<b>3</b> •Cl	$3.1 \times 10^3$	56	55	$8.3 \times 10^3$	$2.3 \times 10^2$	36
<b>3</b> •Br	$1.1 \times 10^3$	53	21	$2.1 \times 10^3$	$2.4 \times 10^2$	9
<b>3</b> •I	$5.1 \times 10^2$	77	7	$4.3 \times 10^2$	$1.3 \times 10^2$	3

[a] As determined by <sup>1</sup>H NMR spectroscopic titrations and analysis of the data using HypNMR software;<sup>[20]</sup> errors are estimated to be no more than  $\pm 15\%$ .

basis ion-pair dissociation was assumed to be negligible (Figures S53–S55 in the Supporting Information). Hence, the titration data was fitted to a 1:1 binding model using HypNMR software,<sup>[20]</sup> considering the pyridinium halide axles as single species. The calculated stability constants are given in Table 1 and are the highest for threading of (*Z*)-**1** and (*Z*)-**2** by **3**-Cl. Overall, the constants become lower with decreasing basicity and increasing size of the counteranion in the order: Cl<sup>-</sup> > Br<sup>-</sup> > I<sup>-</sup>. Presumably the anion-binding pocket formed by the four amide-substituents in the pseudorotaxane structure is able to accommodate the smaller chloride better than the larger bromide and iodide. Expansion of the binding site for the larger anions will likely increase steric interaction between the macrocycle and the axle.<sup>[11a]</sup>

In contrast, <sup>1</sup>H NMR titration studies using the (*E*)-isomers, which were obtained by 385 nm irradiation of the corresponding (*Z*)-isomers, resulted in only minor <sup>1</sup>H NMR spectral changes (Figures S29–S34 and S43–S48 in the Supporting Information). Fitting of the data revealed that in particular macrocycle (*E*)-**1**, but also (*E*)-**2**, had remarkably lower affinity for all the pyridinium halide axles as compared to their respective (*Z*)-isomers (see Table 1). The difference in affinity between isomers was the largest (55-fold) for the combination of **1** and **3**-Cl. The most plausible explanation for the lower threading capability of the (*E*)-isomer with respect to the (*Z*)-isomer is that the pyridinium ring of the axle is less well accommodated by the former isomer due to steric repulsion by the stiff-stilbene unit. This is reflected in the overall higher stability constants observed for the larger (*E*)-**2** as compared to (*E*)-**1**. Interestingly, while enlargement of the macrocycle thus leads to overall stronger complexation, it makes that photochemical isomerization has a smaller effect on the threading and dethreading process, that is, the  $K_{a,Z}/K_{a,E}$  ratios are smaller for **2** than for **1**. Importantly, when tetrabutylammonium chloride was titrated to (*E*)-**1** and (*E*)-**2** (Figures S35–S36 and S49–S50 in the Supporting Information) association constants of  $\sim 30$  M<sup>-1</sup> were determined, which is around half of the  $K_a$  value obtained for the titration of (*E*)-**1** with **3**-Cl. This small difference indicates that the macrocycle and axle components do not significantly interact and hence, that no threading occurs. On the other hand, for (*E*)-**2** the association constant determined for **3**-Cl is almost eight times higher than that of tetrabutylammonium chloride, indicating that here the macrocycle can still be threaded to a certain extent.

To confirm that (de)threading can be controlled in situ by light, photoswitching of the smallest macrocycle (*Z*)-**1** was carried out in the presence of the strongest binding pyridinium chloride axle **3**-Cl. The irradiation process was monitored by <sup>1</sup>H NMR spectroscopy in dichloromethane-*d*<sub>2</sub> (Figures 3 and S56 in the Supporting Information). Starting with the threaded (*Z*)-isomer, 385 nm irradiation led to appearance of the <sup>1</sup>H NMR signals characteristic for the (*E*)-isomer, where subsequent irradiation at 340 nm led to partial recovery of the signals of the original threaded species. The PSS<sub>385</sub> and PSS<sub>340</sub> (*E*/*Z*) ratios were determined as 90:10 and 31:69, respectively. Interestingly, in particular

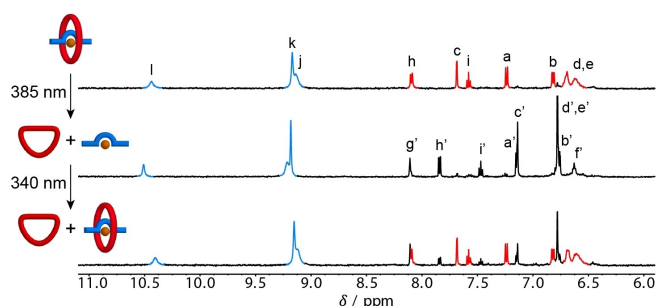


**Figure 3.**  $^1\text{H}$  NMR spectra of a mixture of (*Z*)-**1** and **3-Cl** (1.0 mM and 2.5 mM in dichloromethane- $d_2$ , respectively; top), sequentially irradiated with light of 385 nm (middle) and 340 nm (bottom).

for the latter case, this ratio is thus significantly more biased towards the (*Z*)-isomer than when the macrocycle is irradiated alone ( $\text{PSS}_{340} = 55:45$ , see above).

Unequivocal evidence of pseudorotaxane formation came from single-crystal X-ray crystallography analysis. Suitable single crystals of (*Z*)-**1**⋅**3-Cl** were grown by slow diffusion of diethyl ether into an equimolar mixture of the components in dichloromethane. The solid-state structure shows threading of the macrocycle by the pyridinium axle, where the chloride counteranion is involved in four N(H)⋯Cl and two C(H)⋯Cl hydrogen bonding interactions (distances between 3.256–3.523 Å, see Figure 4 and the Supporting Information for details).<sup>[21]</sup> Furthermore, the axle's electron-poor pyridinium ring is positioned in between the two electron-rich hydroquinone moieties of the macrocycle, indicating a contribution of  $\pi$ - $\pi$  stacking to the overall stability of the pseudorotaxane complex. In addition, the pyridinium methyl group is directed towards the stiff-stilbene ethylene glycol substituents, having electrostatic and possibly also hydrogen-bonding interactions with the oxygen atoms.<sup>[11a]</sup> In this structure, the relative orientation

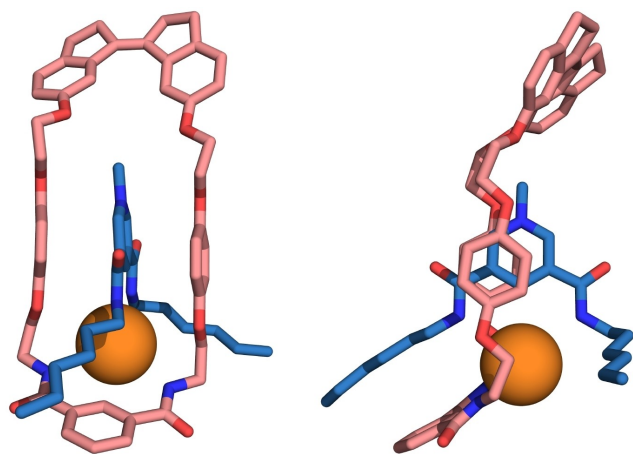
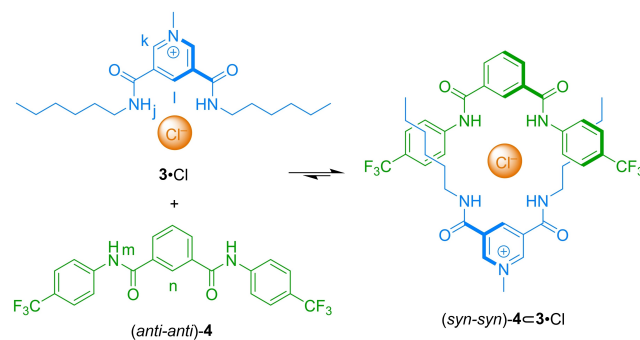


**Figure 4.** Front view and side view of pseudorotaxane (*Z*)-**1**⋅**3-Cl** as found in the crystal structure, shown in stick representation. Co-crystallized diethyl ether and dichloromethane, as well as disorder in the hexyl side chains of the axle component have been omitted for clarity.

of the amide-residues around the chloride ion deflects from perfectly tetrahedral, which is most likely due to packing effects (see Figure S63 in the Supporting Information).

Inspired by the role of messenger molecules in biological signaling processes,<sup>[1]</sup> several efforts have been made to control the transfer of ions and guest molecules between molecular hosts in fully artificial multicomponent supramolecular systems.<sup>[14,15]</sup> Since photoisomerization of the macrocycle in our case led to effective (de)threading, we envisioned light-controlled exchange of the axle subunit between the macrocycle and an appropriate secondary host. To achieve successful axle exchange, the secondary host should ideally have an affinity constant in between that of the (*E*)- and (*Z*)-isomer of the macrocycle.<sup>[15c]</sup> We selected an aromatically substituted isophthalamide derivative since this type of molecule is known to form a heterodimer with **3-Cl** (Scheme 3).<sup>[11a]</sup> By a  $^1\text{H}$  NMR titration experiment in chloroform- $d$  saturated with water, a binding constant for 1:1 complexation of **3-Cl** with *N,N'*-bis(4-(trifluoromethyl)phenyl)isophthalamide (**4**) of  $1.4 \times 10^3 \text{ M}^{-1}$  was determined (Figures S51–S52 in the Supporting Information). This kind of isophthalamide derivative is known to predominantly exist in a *syn-anti* and *anti-anti* conformation in solution,<sup>[22]</sup> which we validated for **4** by DFT energy minimizations on the B3LYP/6-31++G(d,p) level of theory using an IEFPCM dichloromethane solvation model (Tables S3–S6 in the Supporting Information). While the *anti-anti* conformation was found to be lowest in energy, both isomers coexist in solution, which was confirmed by a 1D NOESY experiment (Figure S57 in the Supporting Information). In contrast, complex formation with axle **3-Cl** is only possible in the *syn-syn* conformation, meaning that a net conformational change occurs when forming the heterodimer.<sup>[22]</sup> In the case of light-stimulated pseudorotaxane dethreading and recombination of the axle with isophthalamide **4**, this *syn-anti* conformational change is then coupled in a remote way to macrocycle *E/Z* isomerization.

The stability constant of the **4**⋅**3-Cl** heterodimer lies perfectly in between those determined for complex formation of **3-Cl** with the (*E*)- and (*Z*)-isomer of **1**. As, furthermore, for this macrocycle the largest difference in affinity was obtained, it was selected in combination with secondary host **4** to demonstrate axle exchange. Importantly,



**Scheme 3.** Heterodimer formation between pyridinium chloride axle **3-Cl** and *N,N'*-bis(4-(trifluoromethyl)phenyl)isophthalamide (**4**).

mixing of either (*Z*)-**1** or (*E*)-**1** with **4** did not show significant  $^1\text{H}$  NMR chemical shift changes, as compared to the individual species, corroborating that they do not interact with each other (Figure S58 in the Supporting Information).

When 1 equivalent of axle **3-Cl** was added to isophthalamide **4** in dichloromethane- $d_2$ ,<sup>[23]</sup> the NH ( $H_m$ ) and aromatic singlet ( $H_n$ ) signals of the latter experienced a large downfield shift, indicating dimerization (from  $\delta=8.13$  to 8.91 ppm and from  $\delta=8.45$  to 8.61 ppm, respectively, see Figure 5 and Figures S59–61 in the Supporting Information). These signals, in addition to two signals belonging to the axle (i.e.,  $H_j$  and  $H_k$  at  $\delta=9.42$  and 9.10 ppm, respectively), were therefore used to track the exchange process. When 5 equivalents of (*Z*)-**1** were added to this mixture, the characteristic signals of pseudorotaxane (*Z*)-**1**⋮**3-Cl** appeared, and thus part of the initially formed **4**⋮**3-Cl** complex had dissociated (Figure 5). Break-up of this heterodimer was corroborated by the upfield shifting of aforementioned NH ( $H_m$ ) and aromatic singlet ( $H_n$ ) signals of **4** (from  $\delta=8.91$  to 8.73 ppm and from  $\delta=8.61$  to 8.56 ppm, respectively), as well as of NH ( $H_j$ ) and aromatic proton ( $H_k$ ) signals of **3-Cl** (from  $\delta=9.42$  to 9.08 ppm and from  $\delta=9.10$  to 8.96 ppm, respectively). After irradiation with 385 nm light to trigger conversion from (*Z*)-**1** to (*E*)-**1** (>95%), a downfield shift of all these proton signals was noted to chemical shift values that closely resemble those observed for **4**⋮**3-Cl** before the addition of (*Z*)-**1** (i.e.,  $H_m$ ,  $H_n$ ,  $H_j$  and  $H_k$  shifted to  $\delta=8.91$ , 8.60, 9.34 and 9.04 ppm, respectively). These spectral changes thus indicate almost quantitative dethreading of the axle from the macrocycle upon *Z*→*E* isomerization and concomitant reassembly into the heterodimer, which was expected based on the large difference in stability constant between (*E*)-**1**⋮**3-Cl** and **4**⋮**3-Cl** ( $K_{a,4}/K_{a,(E)-1}=25$ ). When the

mixture was subsequently irradiated with 340 nm light to give a mixture with an (*E*)-**1**/(*Z*)-**1** ratio of approximately 50:50, the regenerated (*Z*)-isomer of the macrocycle recombined with **3-Cl** to form the pseudorotaxane structure, as illustrated by the upfield shifting of the tracked proton signals of the axle ( $H_j$  and  $H_k$ , from  $\delta=9.34$  and 9.04 ppm to  $\delta=9.12$  and 8.97 ppm, respectively), as well as of the secondary host ( $H_m$  and  $H_n$ , from  $\delta=8.91$  and 8.60 ppm to  $\delta=8.77$  and 8.57 ppm, respectively). This 385/340 nm irradiation cycle could be repeated without significant signs of degradation.

To estimate the concentrations of all species present in solution under the experimental conditions used, this four-component system was modeled using HySS software (see Table S1 in the Supporting Information).<sup>[24,25]</sup> Initially, in the equimolar mixture of **4** and **3-Cl**, approximately 30% dimerizes into **4**⋮**3-Cl**. The addition of (*Z*)-**1** increases the total amount of associated axle to 85%, of which the majority is complexed with the macrocycle [(*Z*)-**1**⋮**3-Cl**/**4**⋮**3-Cl** ratio 10:1]. At the PSS<sub>385</sub>, the total amount of bound axle is reduced to 40%, where **4**⋮**3-Cl** now becomes the dominant complex [(*Z*)-**1**⋮**3-Cl**/**4**⋮**3-Cl**=1:2.5]. Finally, in the PSS<sub>340</sub> mixture, containing (*E*)-**1** and (*Z*)-**1** in a 1:1 ratio, an estimated amount of 75% of the axle is bound, primarily by the macrocycle [(*Z*)-**1**⋮**3-Cl**/**4**⋮**3-Cl** 5:1]. This simulation confirms that, upon each step, part of axle **3-Cl** is transferred between macrocycle (*Z*)-**1** and isophthalamide **4**.

## Conclusion

In summary, we have developed photoswitchable stiff-stilbene based macrocycles, of which the (*Z*)-isomer can assemble into stable pseudorotaxane structures with pyridinium halide axles. As the counteranion functions as template, the overall stability of the complex can be tuned (from high to low in the order  $\text{Cl}^- > \text{Br}^- > \text{I}^-$ ). Photoisomerization to the (*E*)-isomer results in remarkably reduced affinity (up to 55-fold) for the axle and hence, dethreading. In addition, when a secondary isophthalamide host is present in the mixture, the axle component is effectively transferred between the macrocycle and this secondary host upon 385/340 nm irradiation. Axle exchange and dual complex formation are thus successfully controlled by light in a multicomponent system. The approach presented here offers new opportunities for biasing the threading direction using nonsymmetric axles (towards molecular pumping).<sup>[5,6]</sup> Further, our results could stimulate the development of future, more complex supramolecular systems that involve signaling, communication, and information processing.<sup>[14,15]</sup>

## Supporting Information

The authors have cited additional references within the Supporting Information.<sup>[26–30]</sup>

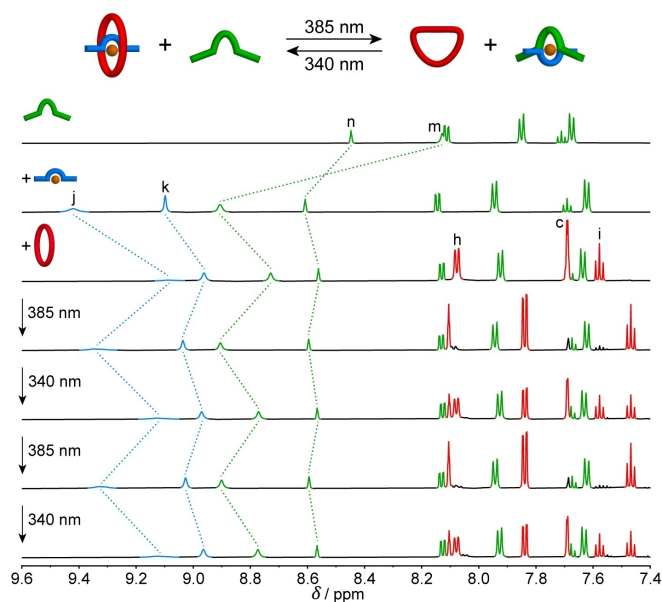


**Figure 5.**  $^1\text{H}$  NMR spectral changes in the aromatic region of **4**, **1**, and **3-Cl** upon mixing the three components in dichloromethane- $d_2$  and sequential irradiation with 385/340 nm light.

## Acknowledgements

Financial support from the European Research Council (Starting Grant no. 802830 to S.J.W.) and the Dutch Research Council (NWO-ENW, Vidi Grant no. VI.Vidi.192.049 to S.J.W.) is gratefully acknowledged. We thank Dr. Karthick B. Sai Sankar Gupta and Alfons Lefebvre for help with NMR experiments.

## Conflict of Interest

The authors declare no conflict of interest.

## Data Availability Statement

The data that support the findings of this study are available in the supplementary material of this article.

**Keywords:** Anions · Molecular Switches · Photochromism · Pseudorotaxanes · Stiff-Stilbene

- [1] F. Marks, U. Klingmüller, K. Müller-Decker, *Cellular Signal Processing: An Introduction to the Molecular Mechanisms of Signal Transduction*, Garland Science, New York, **2009**.
- [2] M. Schliwa, G. Woehlke, *Nature* **2003**, *422*, 759–765.
- [3] a) S. Shinkai, O. Manabe, *Top. Curr. Chem.* **1984**, *121*, 67–104; b) S. Lee, A. H. Flood, *J. Phys. Org. Chem.* **2013**, *26*, 79–86; c) D.-H. Qu, Q.-C. Wang, Q.-W. Zhang, X. Ma, H. Tian, *Chem. Rev.* **2015**, *115*, 7543–7588; d) A. Díaz-MoscOSO, P. Ballester, *Chem. Commun.* **2017**, *53*, 4635–4652; e) J. de Jong, J. E. Bos, S. J. Wezenberg, *Chem. Rev.* **2023**, *123*, 8530–8574; f) C. Ludwig, J. Xie, *ChemPhotoChem* **2023**, *7*, e202300126.
- [4] For selected examples, see: a) S. Shinkai, T. Minami, Y. Kusano, O. Manabe, *J. Am. Chem. Soc.* **1983**, *105*, 1851–1856; b) J.-F. Xu, Y.-Z. Chen, L.-Z. Wu, C.-H. Tung, Q.-Z. Yang, *Org. Lett.* **2014**, *16*, 684–687; c) X. Yan, J.-F. Xu, T. R. Cook, F. Huang, Q.-Z. Yang, C.-H. Tung, P. J. Stang, *Proc. Natl. Acad. Sci. USA* **2014**, *111*, 8717–8722; d) S. T. J. Ryan, J. del Barrio, R. Suardiáz, D. F. Ryan, E. Rosta, O. A. Scherman, *Angew. Chem. Int. Ed.* **2016**, *55*, 16096–16100; e) X. Chi, W. Cen, J. A. Queenan, L. Long, V. M. Lynch, N. M. Khashab, J. L. Sessler, *J. Am. Chem. Soc.* **2019**, *141*, 6468–6472; f) D. Villarón, M. A. Siegler, S. J. Wezenberg, *Chem. Sci.* **2021**, *12*, 3188–3193; g) S. Xiong, Q. He, *Chem. Commun.* **2021**, *57*, 13514–13517; h) P. Sokotowska, K. J. Dąbrowa, S. Jarosz, *Org. Lett.* **2021**, *23*, 2687–2692; i) Y. Liu, Q. Zhang, S. Crespi, S. Chen, X.-K. Zhang, T.-Y. Xu, C.-S. Ma, S.-W. Zhou, Z.-T. Shi, H. Tian, B. L. Feringa, D.-H. Qu, *Angew. Chem. Int. Ed.* **2021**, *60*, 16129–16138.
- [5] For review articles, see: a) V. Balzani, A. Credi, F. M. Raymo, J. F. Stoddart, *Angew. Chem. Int. Ed.* **2000**, *39*, 3348–3391; b) S. Erbas-Cakmak, D. A. Leigh, C. T. McTernan, A. L. Nussbaumer, *Chem. Rev.* **2015**, *115*, 10081–10206; c) Y. Feng, M. O valle, J. S. W. Seale, C. K. Lee, D. J. Kim, R. D. Astumian, J. F. Stoddart, *J. Am. Chem. Soc.* **2021**, *143*, 5569–5591.
- [6] a) H. Li, C. Cheng, P. R. McGonigal, A. C. Fahrenbach, M. Frasconi, W.-G. Liu, Z. Zhu, Y. Zhao, C. Ke, J. Lei, R. M. Young, S. M. Dyar, D. T. Co, Y.-W. Yang, Y. Y. Botros, W. A. Goddard, III, M. R. Wasielewski, R. D. Astumian, J. F. Stoddart, *J. Am. Chem. Soc.* **2013**, *135*, 18609–18620; b) G. Ragazzon, M. Baroncini, S. Silvi, M. Venturi, A. Credi, *Nat. Nanotechnol.* **2015**, *10*, 70–75; c) M. Canton, J. Groppi, L. Casimiro, S. Corra, M. Baroncini, S. Silvi, A. Credi, *J. Am. Chem. Soc.* **2021**, *143*, 10890–10894.
- [7] For review articles, see: a) M. Xue, Y. Yang, X. Chi, X. Yan, F. Huang, *Chem. Rev.* **2015**, *115*, 7398–7501; b) L. Wang, Q. Li, *Chem. Soc. Rev.* **2018**, *47*, 1044–1097; c) A. Credi, S. Silvi, M. Venturi, Light-Operated Machines Based on Threaded Molecular Structures, In *Molecular Machines and Motors. Topics in Current Chemistry, Vol. 354*, Springer, Cham, **2014**.
- [8] For selected examples, see: a) M. Asakawa, P. R. Ashton, V. Balzani, C. L. Brown, A. Credi, O. A. Matthews, S. P. Newton, F. M. Raymo, A. N. Shipway, N. Spencer, A. Quick, J. F. Stoddart, A. J. P. White, D. J. Williams, *Chem. Eur. J.* **1999**, *5*, 860–875; b) V. Balzani, A. Credi, F. Marchioni, J. F. Stoddart, *Chem. Commun.* **2001**, 1860–1861; c) K.-S. Jeong, K.-J. Chang, Y.-J. An, *Chem. Commun.* **2003**, 1450–1451; d) M. Baroncini, S. Silvi, M. Venturi, A. Credi, *Chem. Eur. J.* **2010**, *16*, 11580–11587; e) A. Martínez-Cuevza, F. Morales, G. R. Marley, A. Lopez-Lopez, J. C. Martínez-Costa, D. Bautista, M. Alajarin, J. Berna, *Eur. J. Org. Chem.* **2019**, *2019*, 3480–3488; f) M. Colaço, P. Máximo, A. J. Parola, N. Basílio, *Chem. Eur. J.* **2021**, *27*, 9550–9555; g) X. Zhang, Y.-D. Yang, Z.-H. Lu, L.-J. Xu, J. L. Sessler, H.-Y. Gong, *Proc. Natl. Acad. Sci. USA* **2021**, *118*, e2112973118.
- [9] K. Hirose, Y. Shiba, K. Ishibashi, Y. Doi, Y. Tobe, *Chem. Eur. J.* **2008**, *14*, 981–986.
- [10] For review articles, see: a) J. A. Wisner, P. D. Beer, N. G. Berry, B. Tomapatanaget, *Proc. Natl. Acad. Sci. USA* **2002**, *99*, 4983–4986; b) M. D. Lankshear, P. D. Beer, *Acc. Chem. Res.* **2007**, *40*, 657–668; c) M. S. Vickers, P. D. Beer, *Chem. Soc. Rev.* **2007**, *36*, 211–225.
- [11] For selected examples, see: a) J. A. Wisner, P. D. Beer, M. G. B. Drew, *Angew. Chem. Int. Ed.* **2001**, *40*, 3606–3609; b) M. R. Sambrook, P. D. Beer, J. A. Wisner, R. L. Paul, A. R. Cowley, F. Szemes, M. G. B. Drew, *J. Am. Chem. Soc.* **2005**, *127*, 2292–2302; c) M. D. Lankshear, N. H. Evans, S. R. Bayly, P. D. Beer, *Chem. Eur. J.* **2007**, *13*, 3861–3870; d) M. J. Chmielewski, L. Zhao, A. Brown, D. Curiel, M. R. Sambrook, A. L. Thompson, S. M. Santos, V. Felix, J. J. Davis, P. D. Beer, *Chem. Commun.* **2008**, 3154–3156; e) L. M. Hancock, P. D. Beer, *Chem. Eur. J.* **2009**, *15*, 42–44; f) C. J. Serpell, N. L. Kilah, P. J. Costa, V. Félix, P. D. Beer, *Angew. Chem. Int. Ed.* **2010**, *49*, 5322–5326; g) G. T. Spence, C. Chan, F. Szemes, P. D. Beer, *Dalton Trans.* **2012**, *41*, 13474–13485.
- [12] a) D. H. Waldeck, *Chem. Rev.* **1991**, *91*, 415–436; b) D. Villarón, S. J. Wezenberg, *Angew. Chem. Int. Ed.* **2020**, *59*, 13192–13202.
- [13] For pseudorotaxane structures that comprise of stiff-stilbene in the axle, see: a) Y. Wang, C.-L. Sun, L.-Y. Niu, L.-Z. Whu, C.-H. Tung, Y.-Z. Chen, Q.-Z. Yang, *Polym. Chem.* **2017**, *8*, 3596–3602; b) H. Zhu, L. Shangguan, D. Xia, J. H. Mondal, B. Shi, *Nanoscale* **2017**, *9*, 8913–8917; c) Y. Wang, Y. Tian, Y.-Z. Chen, L.-Y. Niu, L.-Z. Wu, C.-H. Tung, Q.-Z. Yang, R. Boulatov, *Chem. Commun.* **2018**, *54*, 7991–7994.
- [14] For review articles, see: a) A. P. de Silva, *Chem. Asian J.* **2011**, *6*, 750–766; b) R. Bofinger, A. Ducrot, L. Jonusauskaite, N. D. McClenaghan, J.-L. Pozzo, G. Sevez, G. Vives, *Aust. J. Chem.* **2011**, *64*, 1301–1314; c) M. Schmittel, *Chem. Commun.* **2015**, *51*, 14956–14968; d) P. Remón, U. Pischel, *ChemPhysChem* **2017**, *18*, 1667–1677.
- [15] For selected examples, see: a) F. M. Raymo, S. Giordani, *J. Am. Chem. Soc.* **2001**, *123*, 4651–4652; b) S. Silvi, A. Arduini, A. Pochini, A. Secchi, M. Tomasulo, F. M. Raymo, M. Baroncini, A. Credi, *J. Am. Chem. Soc.* **2007**, *129*, 13378–13379; c) D. Ray, J. T. Foy, R. P. Hughes, I. Aprahamian, *Nat. Chem.* **2012**, *4*, 757–762; d) S. Ma, M. M. J. Smulders, Y. R. Hristova, J. K.

- Clegg, T. K. Ronson, S. Zarra, J. R. Nitschke, *J. Am. Chem. Soc.* **2013**, *135*, 5678–5684; e) A. Tron, I. Pianet, A. Martinez-Cuevza, J. H. R. Tucker, L. Pisciotani, M. Alajarin, J. Berna, N. D. McClenaghan, *Org. Lett.* **2017**, *19*, 154–157; f) B. S. Pilgrim, D. A. Roberts, T. G. Lohr, T. K. Ronson, J. R. Nitschke, *Nat. Chem.* **2017**, *9*, 1276–1281; g) J. S. Park, J. Park, Y. J. Yang, T. T. Tran, I. S. Kim, J. L. Sessler, *J. Am. Chem. Soc.* **2018**, *140*, 7598–7604; h) S. Wiedbrauk, T. Bartelmann, S. Thumser, P. Mayer, H. Dube, *Nat. Commun.* **2018**, *9*, 1456; i) I. Paul, A. Ghosh, M. Bolte, M. Schmittel, *ChemistryOpen* **2019**, *8*, 1355–1360; j) A. Ghosh, I. Paul, M. Schmittel, *J. Am. Chem. Soc.* **2019**, *141*, 18954–18957; k) P. Remón, D. González, M. A. Romero, N. Basílio, U. Pischel, *Chem. Commun.* **2020**, *56*, 3737–3740; l) A. Ghosh, I. Paul, M. Schmittel, *J. Am. Chem. Soc.* **2021**, *143*, 5319–5323; m) F. Fratello, F. Tavani, M. Di Berto Mancini, D. Del Giudice, G. Capocasa, I. Kieffer, O. Lanzalunga, S. Di Stefano, P. D'Angelo, *J. Phys. Chem. Lett.* **2022**, *13*, 5522–5529; n) J. Chen-Wu, P. Máximo, P. Remón, A. J. Parola, N. Basílio, U. Pischel, *Chem. Commun.* **2023**, *59*, 3431–3434.
- [16] L. M. Hancock, L. C. Gilday, S. Carvalho, P. J. Costa, V. Félix, C. J. Serpell, N. L. Kilah, P. D. Beer, *Chem. Eur. J.* **2010**, *16*, 13082–13094.
- [17] K.-Y. Ng, V. Felix, S. M. Santos, N. H. Rees, P. D. Beer, *Chem. Commun.* **2008**, 1281–1283.
- [18] S. Akbulatov, Y. Tian, R. Boulatov, *J. Am. Chem. Soc.* **2012**, *134*, 7620–7623.
- [19] Due to the volatile nature of dichloromethane- $d_2$ , the  $^1\text{H}$  NMR titration experiments were performed using chloroform- $d$ , which was saturated with  $\text{H}_2\text{O}$  for consistency across measurements.
- [20] C. Frassinetti, S. Ghelli, P. Gans, A. Sabatini, M. S. Moruzzi, A. Vacca, *Anal. Biochem.* **1995**, *231*, 374–382.
- [21] Deposition number 2268373 [for (Z)-**1**- $\text{C}\equiv\text{C}\cdot\text{Cl}$ ] contains the supplementary crystallographic data for this paper. These data are provided free of charge by the joint Cambridge Crystallographic Data Centre and Fachinformationszentrum Karlsruhe Access Structures service. Both the *P* and *M* enantiomers of macrocycle (Z)-**1** are observed in the crystal lattice (see Figure S62–S63 in the Supporting Information).
- [22] a) K. Kavallieratos, S. R. De Gala, D. J. Austin, R. H. Crabtree, *J. Am. Chem. Soc.* **1997**, *119*, 2325–2326; b) K. Kavallieratos, C. M. Bertao, R. H. Crabtree, *J. Org. Chem.* **1999**, *64*, 1675–1683; c) C. A. Hunter, D. H. Purvis, *Angew. Chem. Int. Ed.* **1992**, *31*, 792–795; d) M. J. Chmielewski, J. Jurczak, *Chem. Eur. J.* **2006**, *12*, 7652–7667.
- [23] The axle exchange experiment was carried out in dichloromethane- $d_2$ , which was more suitable for irradiation studies than chloroform- $d$ , in which slight degradation was observed after multiple switching cycles.
- [24] L. Alderighi, P. Gans, A. Ienco, D. Peters, A. Sabatini, A. Vacca, *Coord. Chem. Rev.* **1999**, *184*, 311–318.
- [25] The association constants used to estimate the distribution of species in the axle exchange experiments were determined in chloroform- $d$ /sat.  $\text{H}_2\text{O}$ . The volatile nature of dichloromethane- $d_2$  did not allow for accurate and reliable titrations.
- [26] J. A. Malla, A. Upadhyay, P. Ghosh, D. Mondal, A. Mondal, S. Sharma, P. Talukdar, *Org. Lett.* **2022**, *24*, 4124–4128.
- [27] A. L. Spek, *Acta Crystallogr. Sect. D* **2009**, *65*, 148–155.
- [28] G. M. Sheldrick, *Acta Crystallogr. Sect. C* **2015**, *71*, 3–8.
- [29] Gaussian 09, Revision D.01, M. J. Frisch, G. W. Trucks, H. B. Schlegel, G. E. Scuseria, M. A. Robb, J. R. Cheeseman, G. Scalmani, V. Barone, B. Mennucci, G. A. Petersson, H. Nakatsuji, M. Caricato, X. Li, H. P. Hratchian, A. F. Izmaylov, J. Bloino, G. Zheng, J. L. Sonnenberg, M. Hada, M. Ehara, K. Toyota, R. Fukuda, J. Hasegawa, M. Ishida, T. Nakajima, Y. Honda, O. Kitao, H. Nakai, T. Vreven, J. A. Montgomery, Jr., J. E. Peralta, F. Ogliaro, M. Bearpark, J. J. Heyd, E. Brothers, K. N. Kudin, V. N. Staroverov, T. Keith, R. Kobayashi, J. Normand, K. Raghavachari, A. Rendell, J. C. Burant, S. S. Iyengar, J. Tomasi, M. Cossi, N. Rega, J. M. Millam, M. Klene, J. E. Knox, J. B. Cross, V. Bakken, C. Adamo, J. Jaramillo, R. Gomperts, R. E. Stratmann, O. Yazyev, A. J. Austin, R. Cammi, C. Pomelli, J. W. Ochterski, R. L. Martin, K. Morokuma, V. G. Zakrzewski, G. A. Voth, P. Salvador, J. J. Dannenberg, S. Dapprich, A. D. Daniels, O. Farkas, J. B. Foresman, J. V. Ortiz, J. Cioslowski, D. J. Fox, Gaussian, Inc, Wallingford CT, **2013**.
- [30] M. D. Hanwell, D. E. Curtis, D. C. Lonie, T. Vandermeersch, E. Zurek, G. R. Hutchison, *J. Cheminf.* **2012**, *4*, 17.

Manuscript received: November 2, 2023

Accepted manuscript online: December 7, 2023

Version of record online: December 7, 2023

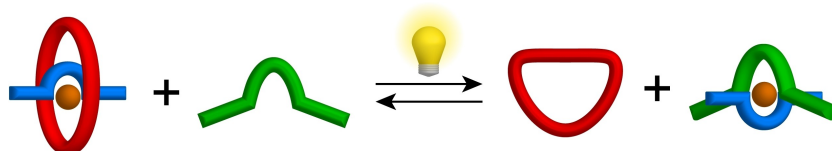


## Research Articles

## Rotaxanes

J. de Jong, M. A. Siegler,  
S. J. Wezenberg\* e202316628

A Photoswitchable Macrocycle Controls  
Anion-Templated Pseudorotaxane Forma-  
tion and Axle Relocalization



Anion-templated pseudorotaxane forma-  
tion is effectively controlled by macro-  
cycles that expand and contract in  
response to a light stimulus. Upon light-  
induced threading and dethreading, the  
axle component can dynamically relocate

between the macrocycle and a secondary  
isophthalamide host. This work is a  
stepping stone towards signal process-  
ing in multicomponent supramolecular  
systems.